

An integral-equation conical solver: some formulas and numerical experiments

Leonid I. Goray

St. Petersburg Physics and Technology Center for Research and Education, Russian Academy of Sciences, Russia and Institute for Analytical Instrumentation, RAS, Russia; e-mail: lig@pcgrate.com

Gunther Schmidt

Weierstrass Institute of Applied Analysis and Stochastics, Germany

We present some formulas derived from the developed boundary integral equation theory, which are important for calculations of the efficiency, absorption, and polarization angles of gratings in conical diffraction. Examples of efficiency computations of x-ray grazing-incidence, high-conductive anomalously absorbing, high-spatial-frequency deep transmission, and cross-polarized symmetrical-groove-profiled gratings are considered. The solver tested has been found universal and accurate for calculating various off-plane diffraction problems.

1 INTRODUCTION

We consider conical (off-plane) diffraction of time-harmonic plane waves by 1D structures. The term '1D' refers to a diffraction grating or a rough mirror having any conductivity on a planar surface in \mathbb{R}^3 , which is periodic in one surface direction, constant in the second, and has an arbitrary border profile including edges and non-functions. For the numerical simulation of conical diffraction by general optical gratings several rigorous methods have been proposed: differential, coordinate transformation, modal, fictitious sources, and finite element methods [1]. In Ref. [2] T-matrix and integral equation methods were described for off-plane transmission and low-conducting sine-profiled gratings. The classical (in-plane) boundary integral equation methods are found to be very efficient to model high-conductive deep-groove gratings in the TM polarization, profile curves with corners, gratings with thin coated layers, randomly rough mirrors and gratings, and diffraction problems at very small wavelength-to-period ratios.

The electromagnetic formulation of conical diffraction by gratings reduces Maxwell equations to a system of two Helmholtz equations in \mathbb{R}^2 , which are coupled by transmission conditions at the interface between different materials and a subject to radiation conditions in the upper and lower mediums. The integral equations obtained using

boundary integrals of the single and double layer potentials including the tangential derivative of single layer potentials interpreted as singular integrals can be found elsewhere [3]. In the case of classical diffraction, when the incident wave vector is orthogonal to the groove (z -) direction, the system degenerates to independent transmission problems for the two basic polarizations of the incident wave, whereas for the case of conical diffraction the boundary values of the z -components as well as their normal and tangential derivatives at the interface are coupled.

In this paper we present some important formulas, including a few new ones, derived from the theory which are expedient for the calculation of the far-field, general polarization properties, and absorption in conical diffraction mounts. Besides, we provide the numerical examples for cases of well known optical applications of conical diffraction, more specifically: shallow gratings working in the x-ray and extreme ultraviolet (EUV) ranges at grazing angles; shallow and deep high-conductive, anomalously absorbing gratings illuminated at near normal and grazing incidence; high-spatial-frequency, deep transmission gratings having high anti-reflection and polarization conversion properties; generalized spectroscopic ellipsometry and scatterometry techniques.

2 DIFFRACTION PROBLEM

The grating is a cylindrical surface whose generatrices are parallel to the z -axis and whose section in the (x, y) -plane is given by the simple, nonintersecting and d -periodic curve Σ , either C^∞ or piecewise C^2 (see Fig. 1). We assume that the open arc Γ denotes one period of Σ . The wavenumber inside $G_+ \times \mathbb{R}$ is denoted by $k^+ = (\alpha, -\beta, \gamma)$ with the

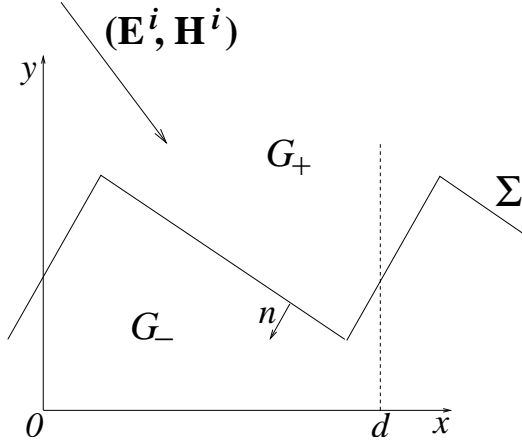


Figure 1: Schematic cross section of a grating.

z -components of the incident time-harmonic field

$$\begin{aligned} u^i(x, y) e^{i\gamma z} &= E_z^i(x, y) e^{i(\alpha x - \beta y + \gamma z)}, \\ v^i(x, y) e^{i\gamma z} &= B_z^i(x, y) e^{i(\alpha x - \beta y + \gamma z)}, \end{aligned}$$

where $\alpha = k^+ \sin \theta^i \cos \phi^i$, $\beta = k^+ \cos \theta^i \cos \phi^i$, $\gamma = k^+ \sin \phi^i$, and $|\theta^i|, |\phi^i| < \pi/2$. The components of the wave vector \mathbf{k}^\pm for $(x, y) \in G_\pm$ satisfy $\beta > 0$ and $(k^\pm)^2 = \omega^2 \varepsilon^\pm \mu^\pm$ with piecewise constant functions of electric permittivity and magnetic permeability $\varepsilon(x, y) = \varepsilon^\pm$ and $\mu(x, y) = \mu^\pm$, respectively. Due to the periodicity of Σ the incident wave is scattered into a finite number of plane waves in $G_+ \times \mathbb{R}$ and also in $G_- \times \mathbb{R}$ if k^- is real. The wave vectors of these outgoing modes lie on the surface of a cone whose axis is parallel to the z -axis. Therefore one speaks of conical diffraction. Classical diffraction corresponds to $\mathbf{k}^+ \cdot \mathbf{e}_z = 0$, whereas $\phi^i \neq 0$ characterizes conical diffraction.

The Maxwell equations imply that the total fields E_z, H_z satisfy the Helmholtz equations in G_\pm

$$(\Delta + (\kappa^\pm)^2) E_z = (\Delta + (\kappa^\pm)^2) H_z = 0,$$

where $(\kappa^\pm)^2 = (k^\pm)^2 - \gamma^2$. It can be shown that under the condition $\kappa \neq 0$, which will be assumed throughout, the components E_z, H_z determine the electromagnetic field (\mathbf{E}, \mathbf{H}) .

By using $H_z = \sqrt{(\varepsilon^+/\mu^+)} B_z = ZB_z$ and the continuity of the tangential components of \mathbf{E} and \mathbf{H} on the surface we can write the jump conditions

in the form

$$\begin{aligned} [E_z]_\Sigma &= [H_z]_\Sigma = 0, \\ \left[\frac{\varepsilon \omega^2 \partial_n E_z}{\kappa^2} \right]_\Sigma &= -\varepsilon^+ \sin \phi \left[\frac{\omega^2 \partial_t B_z}{\kappa^2} \right]_\Sigma, \\ \left[\frac{\mu \omega^2 \partial_n B_z}{\kappa^2} \right]_\Sigma &= \mu^+ \sin \phi \left[\frac{\omega^2 \partial_t E_z}{\kappa^2} \right]_\Sigma, \end{aligned}$$

where $[.]$ denotes the jump of functions on Σ and $\partial_n = n_x \partial_x + n_y \partial_y$ and $\partial_t = -n_y \partial_x + n_x \partial_y$ are the normal and tangential derivatives on Σ , respectively. The z -components of the incoming field

$$E_z^i(x, y) = p_z^i e^{i(\alpha x - \beta y)}, B_z^i(x, y) = s_z^i e^{i(\alpha x - \beta y)} / Z$$

are α -quasiperiodic in x of period d . Here the vector \mathbf{s}^i is orthogonal to the plane spanned by \mathbf{k}^i and the grating normal $\nu = (0, 1, 0)$ and \mathbf{p}^i lies in that plane:

$$\mathbf{s}^i = \mathbf{k}^i \times (0, 1, 0) / |\mathbf{k}^i \times (0, 1, 0)|, \quad \mathbf{p}^i = \mathbf{s}^i \times \mathbf{k}^i / |\mathbf{k}^i|.$$

If $\mathbf{k}^i = (0, -k^+, 0)$, we set $\mathbf{s}^i = (0, 0, 1)$ and hence $\mathbf{p}^i = (1, 0, 0)$. Then, the incident plane wave is given by its polarization angles

$$\begin{aligned} \delta^i &= \arctan[|(\mathbf{E}^i, \mathbf{s}^i)| / |(\mathbf{E}^i, \mathbf{p}^i)|], \\ \psi^i &= -\arg[(\mathbf{E}^i, \mathbf{s}^i) / (\mathbf{E}^i, \mathbf{p}^i)], \end{aligned}$$

where $\delta^i \in [0, \pi/2]$, $\psi^i \in (-\pi, \pi]$. Since \mathbf{E}^i is orthogonal to the wave vector, $(\mathbf{E}^i, \mathbf{k}^i) = 0$, one can decompose \mathbf{E}^i

$$\mathbf{E}^i = (\mathbf{E}^i, \mathbf{s}^i) \mathbf{s}^i + (\mathbf{E}^i, \mathbf{p}^i) \mathbf{p}^i.$$

It is easy to see that for incident or diffracted field components (\mathbf{E}, \mathbf{s}) and (\mathbf{E}, \mathbf{p}) with propagating angles θ and ϕ and $\rho = \cos \phi (\sin^2 \theta \cos^2 \phi + \sin^2 \phi)^{0.5}$

$$\begin{aligned} (\mathbf{E}, \mathbf{s}) &= (E_z \sin \theta + B_z \cos \theta \sin \phi) / \rho, \\ (\mathbf{E}, \mathbf{p}) &= (E_z \cos \theta \sin \phi - B_z \sin \theta) / \rho. \end{aligned} \quad (1)$$

If $\mathbf{k}^i \parallel \nu$, then $(\mathbf{E}^i, \mathbf{s}^i) = E_z^i$ and $(\mathbf{E}^i, \mathbf{p}^i) = -B_z^i$. From (1) under the normalization condition

$$|(\mathbf{E}^i, \mathbf{s}^i)|^2 + |(\mathbf{E}^i, \mathbf{p}^i)|^2 = 1$$

and $\xi = (\sin^2 \theta^i + \cos^2 \theta^i \sin^2 \phi^i)^{0.5}$ we have

$$\begin{aligned} E_z^i &= (\sin \theta^i \sin \delta^i - \cos \theta^i \sin \phi^i \cos \delta^i e^{(i\psi^i)}) / \xi, \\ B_z^i &= (\cos \theta^i \sin \phi^i \sin \delta^i + \sin \theta^i \cos \delta^i e^{(i\psi^i)}) / \xi, \end{aligned}$$

to define an incident plane wave with the given polarization angles δ^i and ψ^i . In the case $\mathbf{k}^i \parallel \nu$ we choose $E_z^i = \sin \delta^i$, $B_z^i = \cos \delta^i e^{(i\psi^i)}$.

The well known outgoing wave conditions are:

$$(E_z, B_z) = (E_z^i, B_z^i) + \sum_{n \in \mathbb{Z}} (E_n^+, B_n^+) e^{i(\alpha_n x + \beta_n^+ y)},$$

for $y \geq H$,

$$(E_z, B_z) = \sum_{n \in \mathbb{Z}} (E_n^-, B_n^-) e^{i(\alpha_n x - \beta_n^- y)},$$

for $y \leq -H$, where $\Sigma \subset \{(x, y) : |y| < H\}$, and α_n, β_n^\pm are given by

$$\alpha_n = \alpha + \frac{2\pi n}{d}, \quad \beta_n^\pm = \sqrt{(\kappa^\pm)^2 - \alpha_n^2}$$

with $0 \leq \arg \beta_n^\pm < \pi$.

In the following it is always assumed that

$$\arg \varepsilon^- \leq 0, \arg \mu^- \leq \pi, \arg (\varepsilon^- \mu^-) < 2\pi,$$

which holds for all existing optical (meta)materials. Then $0 \leq \arg(\kappa^-)^2 < 2\pi$ and β_n^- are properly defined for all n .

Denoting the z -components of the total fields

$$E_z = \begin{cases} u^+ + E_z^i & \text{in } G_+, \\ u^- & \text{in } G_-, \end{cases} \quad B_z = \begin{cases} v^+ + B_z^i & \text{in } G_+, \\ v^- & \text{in } G_-, \end{cases}$$

the problem is defined completely in respect to u^\pm and v^\pm . To transform the transmission problem for the Helmholtz equations in \mathbb{R}^2 to operator boundary integral equations we combined the direct and indirect approach. The function u^-, v^- are represented as the single layer potentials with densities w, τ on Γ

$$\begin{aligned} u^-(P) &= 2 \int_{\Gamma} w(Q) \Psi_{(\kappa^-), \alpha}(P - Q) d\sigma_Q, \\ v^-(P) &= 2 \int_{\Gamma} \tau(Q) \Psi_{(\kappa^-), \alpha}(P - Q) d\sigma_Q, \end{aligned}$$

where $\Psi_{k, \alpha}(P)$, $P = (X, Y)$, is the quasi-periodic fundamental solution of period d given by the infinite series

$$\frac{i}{4} \sum_{n=-\infty}^{\infty} H_0^{(1)} \left(k \sqrt{(X - nd)^2 + Y^2} \right) e^{ind\alpha},$$

As described in [3] the functions w, τ are solutions of the system of integral equations

$$\begin{aligned} \frac{\varepsilon^-(\kappa^+)^2}{\varepsilon^+(\kappa^-)^2} V_\alpha^+ (L_\alpha^- - I) w - (I + K_\alpha^+) V_\alpha^- w \\ + \sin \phi^i \left(1 - \frac{(\kappa^+)^2}{(\kappa^-)^2} \right) H_\alpha^+ V_\alpha^- \tau = 2E_z^i, \\ \frac{\mu^-(\kappa^+)^2}{\mu^+(\kappa^-)^2} V_\alpha^+ (L_\alpha^- - I) \tau - (I + K_\alpha^+) V_\alpha^- \tau \\ - \sin \phi^i \left(1 - \frac{(\kappa^+)^2}{(\kappa^-)^2} \right) H_\alpha^+ V_\alpha^- w = 2B_z^i, \end{aligned} \quad (2)$$

with the boundary operators defined for $P \in \Sigma$ by

$$\begin{aligned} V_\alpha^\pm \varphi(P) &= 2 \int_{\Gamma} \varphi(Q) \Psi_{(\kappa^\pm), \alpha}(P - Q) d\sigma_Q, \\ K_\alpha^\pm \varphi(P) &= 2 \int_{\Gamma} \varphi(Q) \partial_{n(Q)} \Psi_{(\kappa^\pm), \alpha}(P - Q) d\sigma_Q, \\ L_\alpha^- \varphi(P) &= 2 \int_{\Gamma} \varphi(Q) \partial_{n(P)} \Psi_{(\kappa^-), \alpha}(P - Q) d\sigma_Q, \\ H_\alpha^+ \varphi(P) &= 2 \int_{\Gamma} \varphi(Q) \partial_{t(Q)} \Psi_{(\kappa^+), \alpha}(P - Q) d\sigma_Q. \end{aligned}$$

The single and double layer potentials V_α^\pm , K_α^\pm as well as L_α^- appear already in integral methods for classical diffraction. The integral $H_\alpha^+ \varphi$ has to be interpreted as principal value integral, therefore (2) is a system of singular integral equations. The equivalence of the system to the differential formulation of conical diffraction has been shown in [3]. Moreover, the existence and uniqueness of solutions in appropriate function spaces ensure the convergence of numerical methods.

3 ORDERS, EFFICIENCY, AND ABSORPTION

The reflected and transmitted diffraction orders of number n have the wave vectors

$$\begin{aligned} k_n^\pm &= (\alpha_n, \beta_n^\pm, \gamma) \\ &= k^\pm (\sin \theta_n^\pm \cos \phi^\pm, \cos \theta_n^\pm \cos \phi^\pm, \sin \phi^\pm), \end{aligned}$$

with $(k^\pm)^2 - \gamma^2 \geq \alpha_n^2$. Since the z -dependence of all functions is given by $\exp(i\gamma z)$

$$\begin{aligned} \tan \theta_n^\pm &= \mp \alpha_n / \beta_n^\pm = \mp \alpha_n / [(k^\pm)^2 - \gamma^2 - \alpha_n^2]^{0.5}, \\ \phi_n^+ &= \phi^+ = \phi^i, \quad \phi_n^- = \phi^- = \arcsin(k^+ \sin \phi^i / k^-). \end{aligned}$$

By the convention, the outgoing angles θ_n^\pm of the reflected and transmitted orders (to ensure that $\theta_0^+ = -\theta^i$) are taken from the interval $[-\pi/2, \pi/2]$, as well as ϕ^+ and ϕ^- .

The p and s components of the E-fields of the orders are defined similar to those of the incident wave. For a reflected or transmitted order with the wave vector \mathbf{k}_n^\pm polarization angles δ_n^\pm and ψ_n^\pm are determined using (1) for scalar products $(\mathbf{E}_n^\pm, \mathbf{s}_n^\pm)$ and $(\mathbf{E}_n^\pm, \mathbf{p}_n^\pm)$

$$\begin{aligned} \delta_n^\pm &= \arctan[|(\mathbf{E}_n^\pm, \mathbf{s}_n^\pm)| / |(\mathbf{E}_n^\pm, \mathbf{p}_n^\pm)|], \\ \psi_n^\pm &= -\arg[(\mathbf{E}_n^\pm, \mathbf{s}_n^\pm) / (\mathbf{E}_n^\pm, \mathbf{p}_n^\pm)]. \end{aligned}$$

The efficiency of a diffracted order represents the proportion of power radiated in each order. Defining the power as the flux of the Pointing vector

modulus $|\mathbf{P}^i| = \text{Re}(\mathbf{E}^i \times \overline{\mathbf{H}^i})/2$ through a normalized rectangle parallel to the (x, z) -plane, the ratio of the power of a reflected or transmitted propagating order and of the incident wave gives the conical diffraction efficiency η_n^\pm of this order in the simple form (\overline{A} denotes the complex conjugate of A):

$$\eta_n^\pm = (\beta_n^\pm / \beta) (|(\mathbf{E}_n^\pm, \mathbf{s}_n^\pm)|^2 + |(\mathbf{E}_n^\pm, \mathbf{p}_n^\pm)|^2).$$

If $\text{Im } k^- > 0$ then there are no transmitted orders. Thus the usual law of the energy conservation, the sum of efficiencies of all reflected and transmitted orders should be equal to the power of the incident wave, does not hold. Instead, some part of the power is absorbed in the substrate. And such independently calculated heat absorption power plus the power of the reflected orders equals to the power of the incident wave. This requirement is a convenient single computation tool to check the quality of the numerical solution [4]. For the simple grating geometry the absorption power A_{con} can be computed from integrals of the solution of the partial differential formulation of conical diffraction which is derived applying Green's formula [1]:

$$A_{con} = \frac{(\kappa^+)^2}{\beta} \text{Im} \left[\frac{1}{(\kappa^-)^2} \left(\frac{\varepsilon^-}{\varepsilon^+} \int_\Gamma \partial_n E_z \overline{E_z} + \frac{\mu^-}{\mu^+} \int_\Gamma \partial_n B_z \overline{B_z} + 2 \sin \phi^i \text{Re} \int_\Gamma E_z \partial_t \overline{B_z} \right) \right].$$

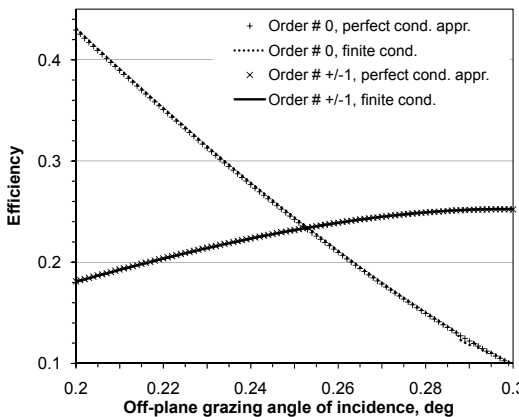


Figure 2: Efficiency of x-ray lamellar grating vs azimuthal grazing incident angle.

4 CONICAL DIFFRACTION EXAMPLES

The numerical implementation approach expedient for the calculation of far-fields and polarization

properties of conical diffraction by gratings and diverse numerical tests devoted to comparing, convergence, accuracy, computation time, and obtaining results for an important case were described in Ref. [1]. Here we present the numerical experiments taken from various optical applications of conical diffraction.

4.1 X-ray-EUV grazing incidence gratings

The conical diffraction mounting in which the direction of incident light is confined to a plane parallel to the direction of the grooves has the unique property of maintaining high and sustained diffraction efficiency that is very important in the x-ray—EUV range. Such gratings are utilized as dispersive elements in laboratory and space spectral instruments, time-delayed compensators or splitters, and spectral purity filters [5, 6, 7, 8].

In Fig. 2 the absolute efficiency in the 0-th and ± 1 -st diffraction orders of the Pt 5000 /mm lamellar symmetrical-profile grating with $2H = 3.7$ nm is calculated for the TE polarized incidence radiation with $\lambda = 0.1$ nm and $\theta^i = 0$ as a function of the azimuthal grazing angle. As one can see in Fig. 2, for the defined azimuthal grazing angle of $\sim 0.25^\circ$ the efficiency are close for three orders simultaneously. Besides, the results obtained for the finite conductivity are very close to those of the perfect conductivity approximation multiplied by Fresnel reflectances [1].

4.2 Anomalously absorbing gratings

Resonance and non-resonance anomalies differing in their nature can be effectively explored in high conductive gratings, such as: surface plasmon excitations, Brewster and Bragg conditions, groove shape features, etc [9, 10, 11, 12]. Because of the s and p modes in conical diffraction being coupled through the boundary conditions, the associated problems are more general, and gratings act as perfect absorbers and local-field enhancers.

In Fig. 3. the absorption of the Ag sine grating with $d = 2.2\mu\text{m}$ and $2H = 100$ nm is calculated for the TE and TM polarized incidence light with $\lambda = 663$ nm as a function of θ^i for $\phi^i = 0$ (in-plane) and $\phi^i = 50^\circ$ (conical). For in-plane diffraction the anomalous absorption exists only for the TM polarization, while for conical diffraction the both components are absorbed but in smaller amounts.

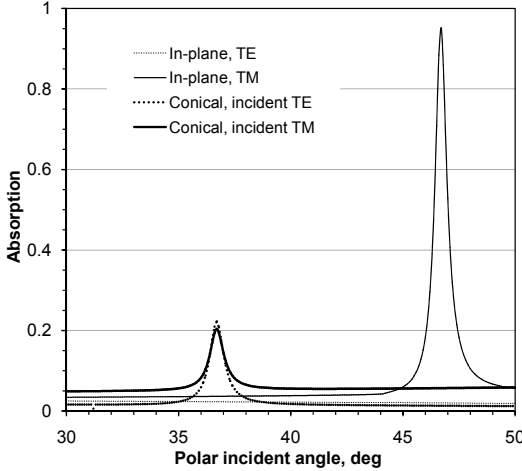


Figure 3: Absorption of conductive sine grating vs polar incident angle.

4.3 Deep transmission gratings

High anti-reflection and polarization conversion properties of gratings are used widely for applications as antireflection surfaces. Such gratings are also used as color filters, artificial dielectrics, beam splitters, wave-plate-type devices, and as their combinations [13, 14].

In Fig. 4. the efficiency in the -1 -st Bragg transmitted order of the dielectric ($(\varepsilon^-)^{0.5} = 1.52$) symmetrical triangle 1- μm -period grating with $2H = 2.3\mu\text{m}$ is calculated for the TE and TM polarized incidence light with $\lambda = 1 \mu\text{m}$ as a function of θ^i for $\phi^i = 0$ (in-plane) and $\phi^i = 27.1^\circ$ (conical). For in-plane diffraction the TE and TM transmitted efficiencies differ significantly, while for conical diffraction the both components are close and high due to the conversion properties.

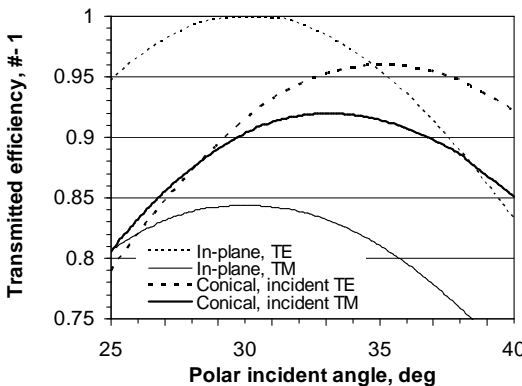


Figure 4: Efficiency of dielectric triangle grating vs polar incident angle.

4.4 Ellipsometry and scatterometry

For ellipsometric scatterometry with an arbitrary azimuth angle the Jones matrix is not diagonal and additional information is available on the grating groove shape, but a generalized ellipsometer, or a Mueller polarimeter, are necessary to retrieve all of the information contained [15, 16]. Solution of the inverse problem to reconstruct the groove shape from a measured diffraction pattern in scatterometry is more complicated in a conical case, however it may also provide additional information on the structure parameters.

In Fig. 5. the amplitude cross-polarization components of the 0-th reflected order of the trapezoidal transmission grating ($\varepsilon^- = 4$) with $d = 360 \text{ nm}$, the top width of 180 nm , and $2H = 180 \text{ nm}$ are calculated for the TE and TM polarized incidence light with $\lambda = 632.8 \text{ nm}$ and $\phi^i = 30^\circ$ as a function of θ^i . For off-plane diffraction the TE and TM 0-order reflected amplitude components are equal for symmetrical groove profiles that approves the validation of the code and the accuracy of computations. In Fig. 6 the good coincidence is demonstrated also for the phases of this example.

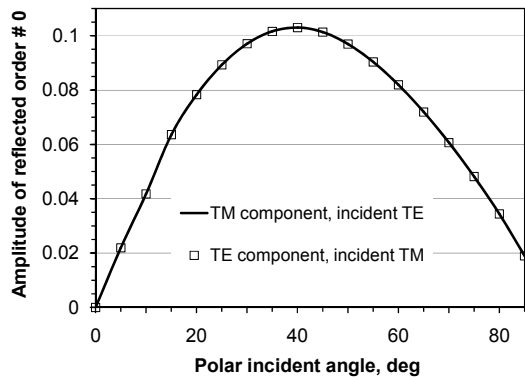


Figure 5: Amplitudes of dielectric trapezoidal grating vs polar incident angle.

5 CONCLUSION

We presented some formulas derived from the developed boundary integral equation theory, which are important for calculations of the efficiency, absorption, and polarization angles of general 1-D gratings in conical diffraction. Examples of efficiency computations of x-ray grazing-incidence, high-conductive anomalously absorbing, high-spatial-frequency deep transmission, and cross-polarized

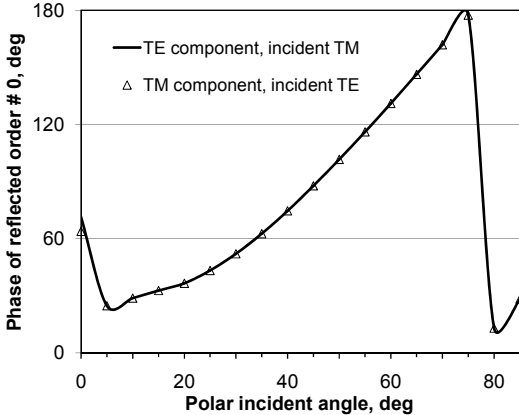


Figure 6: Phases of dielectric trapezoidal grating vs polar incident angle.

symmetrical-groove-profiled gratings were considered. The solver developed and tested has been found universal and accurate for calculating various off-plane diffraction problems for cases of high-conducting, deep groove, and small wavelength-to-period ratio periodical structures including borders with edges.

REFERENCES

- [1] Goray L.I. & Schmidt G., 2009, Solving conical diffraction with integral equations, submitted to *J. Opt. Soc. Am. A*.
- [2] Tsang L., Kong J.A., Ding K.-H. & Ao C.O., 2001, Scattering of Electromagnetic Waves: Numerical Simulations, *Wiley Series in Remote Sensing*, pp. 61–110.
- [3] Schmidt G., 2010, Boundary Integral Methods for Periodic Scattering Problems, *Around the Research of Vladimir Maz'ya II. Partial Differential Equations*, pp. 337–364.
- [4] Goray L.I., Kuznetsov I.G., Sadov S.Yu. & Content D.A., 2006, Multilayer resonant subwavelength gratings: effects of waveguide modes and real groove profiles, *J. Opt. Soc. Am. A*, **Vol. 23,1**, pp. 155–165.
- [5] Seely J.F., Goray L.I., Kjornrattanawanich B., Laming J.M., Holland G.E., Flanagan K.A., Heilmann R.K., Chang C.-H., Schattenburg M.L. & Rasmussen A.P., 2006, Efficiency of a grazing-incidence off-plane grating in the soft-x-ray region, *Appl. Opt.* **Vol. 45,8**, pp. 1680–1687.
- [6] Poletto L., Villoresi P., Benedetti E., Ferrari F., Stagira S., Sansone G. & Nisoli M., 2008, Temporal characterization of a time-compensated monochromator for high-efficiency selection of extreme-ultraviolet pulses generated by high-order harmonics, *J. Opt. Soc. Am. B*, **Vol. 25,7**, pp. B44–B49.
- [7] Goray L.I., 2008, Grazing Incidence Off-Plane Lamellar Grating as a Beam Splitter for a 1-A Free Electron Laser, *J. Surf. Inv. X-ray, Synch. & Neutr. Tech.*, **Vol. 2,5**, pp. 796–800.
- [8] Goray L.I., 2006, Off-plane grazing-incidence fan-groove blazed grating to serve as a high-efficiency spectral purity filter for EUV lithography, *Proc. SPIE*, **Vol. 6317**, p. 63170O.
- [9] Dutta Gupta S., 1987, Theoretical study of plasma resonance absorption in conical diffraction, *J. Opt. Soc. Am. B*, **Vol. 4,11**, p. 1893.
- [10] Mashev L.B., Popov E.K. & Lowen E.G., 1988, Total absorption of light by a sinusoidal grating near grazing incidence, *Appl. Opt.*, **Vol. 27,1**, pp. 152–154.
- [11] Mashev L.B., Popov E.K. & Lowen E.G., 1989, Brewster effects for deep metallic gratings, *Appl. Opt.*, **Vol. 28,13**, pp. 2538–2541.
- [12] Popov E., Tsonev L. & Maystre D., 1994, Lamellar metallic grating anomalies, *Appl. Opt.*, **Vol. 33,22**, pp. 5214–5218.
- [13] Brundrett D.L., Glytsis E.N. & Gaylord T.K., 1994, Homogeneous layer models for high-spatial-frequency dielectric surface-relief gratings: conical diffraction and antireflection designs, *Appl. Opt.*, **Vol. 33,13**, pp. 2695–2706.
- [14] Abe M. & Koshiba M., 1994, Three-dimensional diffraction analysis of dielectric surface-relief gratings, *J. Opt. Soc. Am. A*, **Vol. 11,7**, pp. 2038–2044.
- [15] Novikova T., Martino A., Hatit S. B. & Drevillon B., 2006, Application of Mueller polarimetry in conical diffraction for critical dimension measurements in microelectronics, *Appl. Opt.*, **Vol. 45,16**, pp. 3688–3697.
- [16] Logofatu A.C., Coulombe S.A., Minhas B.K. & McNeil J.R., 1999, Identity of the cross-reflection coefficients for symmetric surface-relief gratings, *J. Opt. Soc. Am. A*, **Vol. 16,5**, pp. 1108–1114.